The Infrared Investigation on the SuperCam Instrument for the Mars2020 Rover. T. Fouchet[1], F. Montmessin[2], O. Forni[3], S. Maurice[3], R.C. Wiens[4], J.R. Johnson[5], S.M. Clegg[1], P. Beck[6], F. Poulet[7], O. Gasnault[3], P.-Y. Meslin[3], and the SuperCam Team. [1]Observatoire de Paris, LESIA, Meudon (thierry.fouchet@obspm.fr); [2]LATMOS, Paris; [3]IRAP, Toulouse; [4]LANL; [5]APL/JHU; [6]IPAG, Grenoble; [7]IAS, Orsay.

Introduction: The Mars2020 Science Definition Team (SDT) has highlighted the need for both context and fine-scale mineralogy to address the Mission Science Objectives A and B of deciphering the geological processes and history of an astrobiologicaly relevant ancient environment on Mars, and assessing the biosignature preservation potential of this environment. The SDT particularly emphasized the need for this mineralogy measurement to be nested and co-aligned with context imaging and fine-scale elemental chemistry.

SuperCam on Mars 2020 is a suite of four instruments that provide these critical observations via Laser Induced Breakdown Spectroscopy (LIBS), Raman spectroscopy [1], visible and near-infrared spectroscopy (VISIR), and high resolution color imaging, all co-aligned and at micro-radian angular resolution. Here we describe the scientific objectives, the technical implementation and performances of the SuperCam infrared investigation.

Scientific Rationale: Orbital infrared spectroscopy has completely revolutionized our concept of the Martian history and particularly demonstrated the presence in the past of persistent liquid water at or near the surface of the planet. Indeed, the two infrared instruments, OMEGA on board the Mars Express spacecraft, and CRISM on board the MRO spacecraft have definitively identified phyllosilicates [2,3], sulfates [4,5], carbonates [6], and zeolites [7,8]. Orbital infrared spectroscopy has also been very successful in identifying various igneous minerals [9], mostly within mafic rocks with low silica contents, but also some rare examples of anorthosites [10]. Infrared spectroscopy is also very sensitive to organics, even if none have been detected so far on the surface of Mars using this technique. Finally, atmospheric dust, CO_2 and H_2O clouds can be efficiently detected and monitored at infrared wavelengths [11].

Orbital instruments have globally characterized the mineralogy of the Martian surface, but have been limited in their spatial resolution to > 20 meters per pixel. The Mars2020 rover will bring down this spatial resolution to 1.3 mm at 2 m distance from the rover to completely identify the mineralogy of outcrops, and to determine the occurrence and distribution of various minerals within the scene. In synergy with context imaging, this will allow to better understand the formation and alteration of the landing site, and participate to the selection of potential biominerals and cached samples. Moreover, SuperCam LIBS will partially clear away dust coatings on surfaces within the IR FOV to maximize the infrared spectroscopy identification power.

Scientific requirements:

Wavelength range. The LIBS laser operates at 1064 nm on SuperCam, capitalizing on ChemCam's high heritage telescope design rejecting the laser light. By operating the instrument in passive mode (no laser) this will allow collection of data in the ~0.4-0.9 µm wavelength range to assist in the identification of iron-bearing minerals [12].

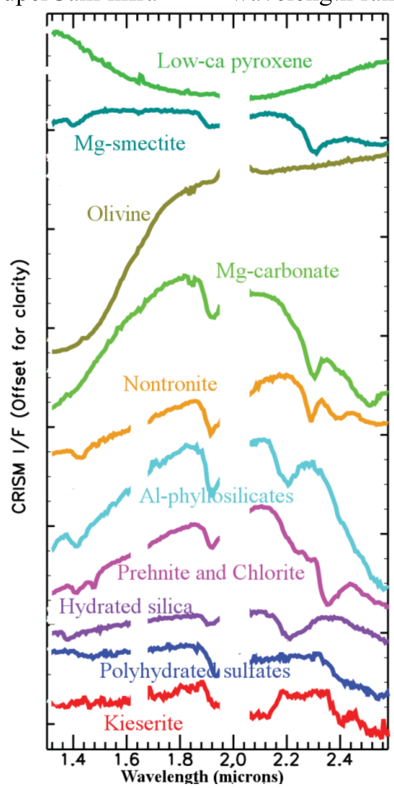

Fig.1 Mineral signatures within the SuperCam IR range. Data from CRISM [13].

The SuperCam IR spectrometer has been designed to work in the 1.3-2.6 µm wavelength range to identify the following minerals : i) Ortho- and chain silicates through Fe-related crystal field bands around 1.0 and 2.0 µm, the latter discriminating pyroxene from olivine; ii) hydrated silicates (mostly phyllosilicates), through the first harmonics of the fundamental vibrational mode of hydroxyl radical OH (1.4 µm) and through the transverse vibrational modes of Al-OH (2.2 µm), Mg/Fe-OH (2.28-2.35 µm) and SiOH (2.20-2.5 µm) ; iii) sulfates (mono- and polyhydrated) through combinations and overtones of OH^- or H_2O bending and stretching fundamentals (1.4 µm, 1.9 µm) and $3\nu_3(SO_4)_2$–overtone (2.4 µm) ; iv) carbonates through overtones and combinations of C-O stretching and bending vibrations ($3\nu_3$ at 2.3 µm and ($\nu_1 + 2\nu_3$) at 2.5 µm), v) complex organic compounds from absorptions at 1.7 and 2.3-2.5 µm due to various combinations of CH_2 and CH_3 asymmetric and symsymmetric stretch.

Spectral resolution and signal-to-noise ratio. These two requirements are closely intertwined in the need to fully resolve the absorption bands and determine accurately their center position to discriminate the structure of various minerals. Following [14], we chose to set a constant 30 cm^{-1} FWHM within the full spectral range (i.e. 5 nm at 1.3 µm, 10 nm at 1.82 µm, and 20 nm at 2.6 µm), while achieving a SNR of 100:1 for a solar zenith angle of 30° at Mars aphelion on 0.3 lambertian albedo in 150 ms of integration per spectral element.

Spatial resolution: To capitalize on the ChemCam heritage, the telescope and the optical fiber design will remain identical in SuperCam. This design sets an angular FOV of 0.67 mrad for the IR spectrometer, translating to a spatial FOV of 6.7 cm at 10 meters, within the SDT requirements for context mineralogy and 1.3 mm at 2 meters, close to the 0.5 mm SDT requirement for fine scale mineralogy.

Calibration Accuracy: The IR spectrometer must account for time-dependent, wavelength-dependent variations in solar illumination as it is filtered by atmospheric aerosols and gases. To prevent artifacts from this variable environment to affect the mineralogical identification enabled by the high SNR, a calibration target mounted on the deck of the rover will realize a relative calibration accuracy of 1% in radiance.

Investigation design: The SuperCam IR spectrometer is based on the SPICAM-IR spectrometer on Mars Express [15]. It is an independent device, linked to the telescope objective by a 300 µm core fiber (length < 20 cm, ChemCam connectors, multi-mode fiber, 0.12 numerical aperture). This optical fiber link requires the IR spectrometer to be mounted on the Mast Unit to maximize the transmission. A radio-frequency (RF) signal drives a transducer, which is attached to the side of an Acousto-Optical Tunable Filter (AOTF). Thus, for each frequency of the piezo, a single wavelength is selected and scattered by ±4° (2 polarizations). The main beam is rejected, while both polarizations are registered by two HgCdTe (MCT) photodiodes and summed (Fig. 2). These MCTs are packaged with a triple-stage TEC. The spectrometer is mounted directly on the SuperCam Optical Box to passively minimize its temperature. The detector TEC can lower the photodiode temperature up to 70°C below that of the spectrometer (verified in the laboratory), although a smaller delta is required usually. The RF driver is designed to independently address 256 wavelengths equally spaced at 15 cm^{-1} to achieve the Nyquist sampling of the AOTF 30-cm^{-1} spectral window.

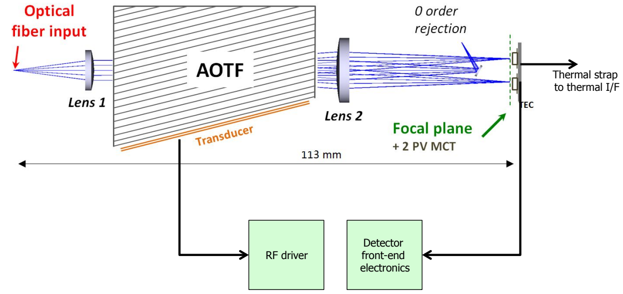

Fig.2 IR spectrometer optical path

Considering the heritage and the simplicity of the design, the IR spectrometer provides extremely valuable science, especially at far distances, using minimal resources (mass of 600 g and volume of 140×56×45 mm^3, see Fig. 3).

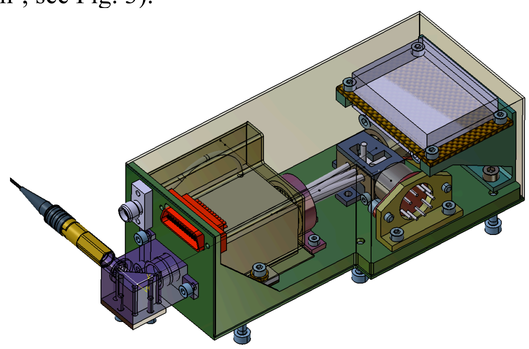

Fig. 3: Mechanical design of IR spectrometer

The spectral scanning flexibility of the SuperCam IR spectrometer will allow various operation modes. The scan mode will perform 30° exploration in azimuth of limited spectral bands to explore the mineralogical diversity of the scene, while raster and fine scale modes will explore the full spectral range of specific targets.

References: [1] Clegg S.M. et al (2015), this meeting. [2] Poulet F. et al. 2005. *Nature 438*, 623. [3] Mustard J.F. et al. (2008) *Nature 454*, 309. [4] Gendrin A. et al. (2005). *Science 307*, 1587. [5] Carter J. (2013) *JGR 118*, 831. [6] Ehlmann B.L. et al. (2008) *Science 322*, 1828. [7] Ehlmann B.L. et al. (2009) *JGR 114*, E00D08. [8] Loizeau D. et al. (2012) *Icarus 219*, 476. [9] Mustard J.F. et al. (2005). *Science 307*, 1594. [10] Carter J. and Poulet F. (2013). *Nature Geoscience 6*, 1008. [11] Wolff M. et al. (2015) in *The Atmosphere and Climate of Mars*. Cambridge University Press. [12] Johnson J.R. et al. (2015) *Icarus*, http://dx.doi.org/10.1016/j.icarus.2014.02.028. [13] Ehlmann B.L. and Edwards, C. (2014) *AREPS 42*, 291. [14] Swayze G.A. et al (2003) *JGR 108*, 5105. [15] Bertaux J.-L. et al. (2000) *PSS 48*, 1303.